eISSN: 3031-9471 | pISSN: 3032-7245 | DOI: 10.69606/geography.v3i3.311

Pubsains Journal of Geographical Sciences and Education

https://journal.pubsains.com/index.php/jgs

[Research Article]

Check for updates

Inferences on the Geological History Through Soil Minerology, Palakkad Gap Region, South India

Jincy Peedamparammal[1,*], Pankajakshan Pangunny[1], Ramachandran Chandran[2], Jeena Beena Sajikumar[1], Sathish Chothodi[3], Dhanya Vijayan[4], Richard Scaria[1]

[1]*Department of Geography, Government College Chittur, Palakkad, Kerala, India*
[2]*Department of Geology, Periyar University, Salem-11, Tamil Nadu, India*
[3]*Department of General and Applied Geography, Doctor Harisingh Gour Vishwavidyalaya (A Central University) Sagar, Madhya Pradesh, India*
[4]*Leibniz Centre for Agricultural Landscape Research (ZALF), Muncheberg, Germany*
[*]*Correspondance: jincykzd@gmail.com*

Article Info:

Received:
19 August 2025

Accepted:
19 September 2025

Published:
23 September 2025

Keywords:
soil mineralogy;
X-ray diffraction;
Palakkad gap.

Abstract

This study assess soil mineralogy and prevailing weathering conditions within the Palakkad Gap, 22 surface soil samples (0–25 cm depth) were collected based on geology, geomorphology, lineament patterns, and land use. Samples were analyzed using X-ray diffraction (XRD; model 600) to determine mineralogical composition (Moore & Reynolds, 1997). The diffraction patterns indicated the presence of quartz, feldspar, kaolinite–illite, gibbsite, goethite, mica, chlorite, calcite, and vermiculite. Quartz and feldspar were interpreted as lithogenic minerals derived from the parent rock, whereas kaolinite, gibbsite, and goethite represent pedogenic weathering products formed under variable pH regimes. Thin-section petrography revealed altered feldspar margins and fractures infilled with Fe-oxides, indicating early to moderate stages of chemical weathering. Mineralogical assemblages in the Palakkad Gap reflect the combined effects of lithology, climate, and geomorphic processes on soil and landscape evolution (Ollier & Pain, 1996; Birkeland, 1999).

Informasi Artikel:

Diterima:
19 Agustus 2025

Disetujui:
19 September 2025

Dipublikasi:
23 September 2025

Kata kunci:
mineralogi tanah;
X-ray diffraction;
Palakkad gap.

Abstrak

Penelitian ini menilai mineralogi tanah dan kondisi pelapukan yang dominan di Palakkad Gap melalui 22 sampel tanah permukaan (kedalaman 0–25 cm) yang dikumpulkan berdasarkan geologi, geomorfologi, pola kelurusan, dan penggunaan lahan. Sampel dianalisis menggunakan X-ray diffraction (XRD; model 600) untuk menentukan komposisi mineral (Moore & Reynolds, 1997). Pola difraksi menunjukkan keberadaan kuarsa, feldspar, kaolinit-ilit, gibbsit, goetit, mika, klorit, kalsit, dan vermikulit. Kuarsa dan feldspar diinterpretasikan sebagai mineral litogenik yang berasal dari batuan induk, sedangkan kaolinit, gibbsit, dan goetit merupakan produk pelapukan pedogenik yang terbentuk di bawah rezim pH yang bervariasi. Petrografi irisan tipis menunjukkan tepian feldspar yang teralterasi dan rekahan yang terisi oksidasi Fe, menandakan tahap awal hingga sedang pelapukan kimia. Rangkaian mineralogi di Palakkad Gap mencerminkan efek gabungan litologi, iklim, dan proses geomorfik pada evolusi tanah dan lanskap (Ollier & Pain, 1996; Birkeland, 1999).

INTRODUCTION

Soil minerals exert a significant influence on their surrounding environment, integrating signals from prevailing climatic conditions during their formation (Rothacker et al., 2018; Hack, 2019). These minerals are products of weathering processes, driven by the combined action of the atmosphere, hydrosphere, and biosphere on rock materials, and they serve as proxies for reconstructing geological history through soil evolution studies (Mukherjee, 2022). Mineral assemblages in soils may be authigenic, formed in situ from local bedrock, or detrital, transported from distant parent material sources (Mukherjee, 2022).

The mineralogical composition of soils is a fundamental attribute that governs their physical, chemical, and biological properties, thereby influencing agricultural productivity and ecosystem functioning (Corwin, 2021). Soil mineralogy not only reflects the characteristics of the parent material but also provides valuable insights into past climatic regimes and the transitions from paleoclimates to present-day conditions (Geiss et al., 2008). From a pedogenic perspective, minerals are typically classified as primary those inherited from the parent rock with minimal structural or chemical alteration since crystallization or secondary, which result from the transformation or recrystallization of primary minerals via chemical weathering under ambient conditions (Wilson, 1999; Dixon & Schulze, 2002).

The occurrence and distribution of secondary minerals, often clay-sized in nature, are strongly influenced by seasonal hydrological variations, water table depth, topographic setting, and regional geology (Chamley, 1989). In humid tropical environments such as Kerala, primary minerals, typically concentrated in the sand and silt fractions, coexist with secondary clay minerals formed through prolonged weathering. Topographic control further enhances soil profile development, promoting the formation of mineralogically diverse horizons that encapsulate the interplay between lithology, geomorphic position, and climate-driven soil-forming processes (Birkeland, 1999).

Thin-section petrographic analysis of weathered rocks and soil materials is a valuable approach for assessing the degree and nature of weathering within pedogenic profiles (Graham et al., 1994; Stoops & Schaefer, 2018). During the weathering process, the particle size of primary minerals progressively decreases, and secondary minerals become concentrated predominantly within the clay and fine-silt fractions. These secondary minerals include aluminosilicates, oxides and hydroxides, carbonates, sulfates, and amorphous phases (Karathanasis et al., 2005). In soils, such alteration products frequently occur as interstratified clays, including kaolinite–illite, kaolinite–vermiculite, and kaolinite–smectite, whose formation is closely linked to prevailing climatic and hydrological conditions.

Soil mineral characterization commonly employs techniques such as X-ray diffraction (XRD) (Zhou et al., 2018; Hamed et al., 2021), as well as thermal, elemental, and optical analyses (Karathanasis et al., 2005). The XRD analysis, in particular, is widely recognized for its ability to provide quantitative mineralogical data and to reconstruct weathering histories (Kahle et al., 2002; Hemming, 2007; Chipera & Bish, 2013). The diffraction pattern of each mineral exhibits a distinctive arrangement of reflections, analogous to a unique fingerprint, allowing precise mineral identification.

This study examines how the geomorphic characteristics of the low-altitude Palakkad Gap influence pedogenesis and how its role as a transitional boundary in atmospheric circulation between Kerala and Tamil Nadu affects soil mineralogy The mineralogical assemblage is primarily governed by the lithology of the underlying rock formations, while soil series classification provides a framework for categorizing the compositional and textural attributes associated with specific soil-forming environments.

METHOD

Study Area and Geological Settings

The Palakkad Gap, a prominent geomorphic feature of the Southern Western Ghats, represents a low-altitude mountain pass situated between the Nilgiri Hills to the north and the Anaimalai–Palni Hills to the south. Geographically, it extends between approximately 10°31’ – 10°53’ N and 76°38’ – 77°00’ E, covering an area of about 979.81 km², of which 52.4% lies within Palakkad District, Kerala, and the remainder in Coimbatore District, Tamil Nadu (Figure 1). The gap functions as a physiographic and climatic transition zone, marked by a pronounced

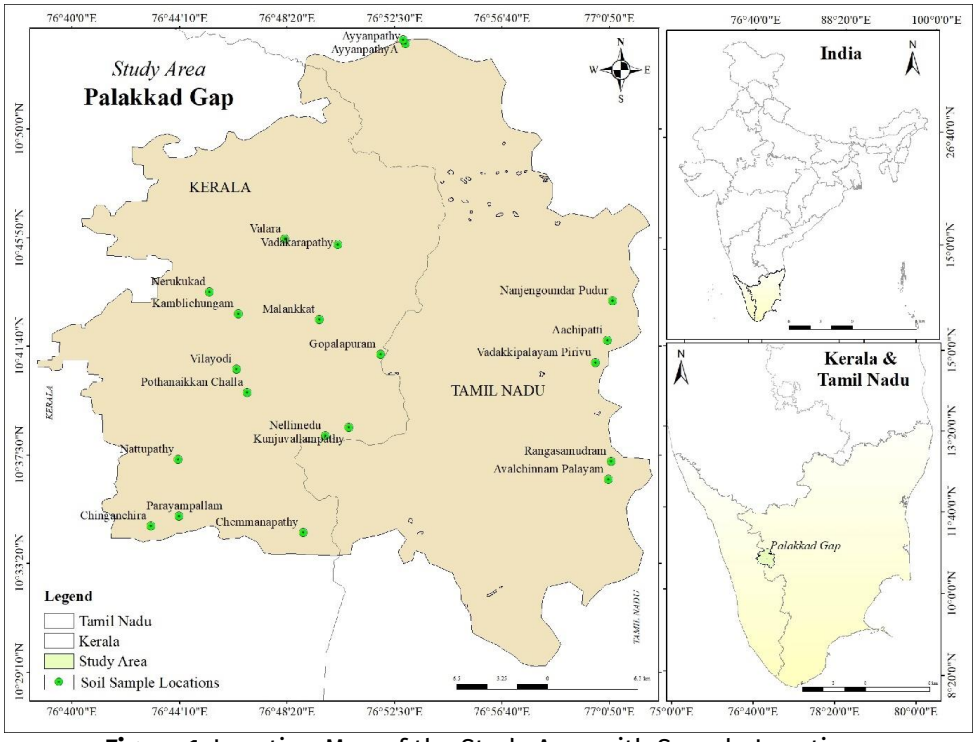

Figure 1. Location Map of the Study Area with Sample Locations
The Study Area Falls between the States of Kerala and Tamil Nadu

gradient in aridity from the humid western slopes to the comparatively drier eastern plains (Hammond, 1964; Verstappen, 1983). The general elevation ranges from 100 to 280 m above mean sea level, with the terrain comprising undulating to rolling plains interspersed with inselbergs, alluvial plains, floodplains, and river terraces. This corridor serves as a critical conduit for atmospheric circulation between the Arabian Sea and the Bay of Bengal, influencing rainfall distribution, soil formation, and land-use patterns in the adjoining regions (Pike & Wilson, 1971). Its unique geological setting, underlain by varied lithologies including charnockite, gneiss, and granitic intrusions, combined with differential weathering and erosional processes, makes the Palakkad Gap an ideal natural laboratory for studying interactions between geology, geomorphology, climate, and pedogenesis.

Climate

Climatically, Kerala experiences a humid tropical regime characterized by high annual precipitation (~3500 mm) and a bimodal rainfall distribution associated with both the southwest (June–September) and northeast (October–November) monsoons (Gadgil, 2003; IMD, 2020). The mean annual temperature is approximately 27°C, with relatively small seasonal variation due to its low-latitude maritime setting. In contrast, the eastern sector of the study area, lying within the western part of Coimbatore District, Tamil Nadu, exhibits a hot and sub-humid to semi-arid climate, receiving substantially lower annual rainfall (~952 mm) primarily during the northeast monsoon. On average, Palakkad District records an annual precipitation of ~2362 mm, reflecting its position on the leeward side of the Western Ghats yet still benefiting from southwest monsoonal inflow through the Palakkad Gap (Pisharoty & Asnani, 1957).

The Palakkad Gap extends from the western edge of the Coimbatore Plateau, particularly from Pollachi Taluk, eastwards into Kerala's Palakkad District. The regional slope exhibits a gentle westward gradient, facilitating the east-west drainage pattern. The Bharathapuzha River, the principal fluvial system within the study area, originates in the eastern highlands and flows westward, following the general slope through the gap before debouching into the Arabian Sea. The regional weather patterns are significantly modulated by the geomorphic configuration, which acts as a low-altitude atmospheric corridor influencing monsoonal wind penetration, rainfall distribution, and associated hydrological regimes across the adjoining states.

Geology

The Palakkad Gap is the only major topographic break approximately 30 km wide with a low mean elevation of ~140 m within the otherwise continuous north–south alignment of the Western Ghats (D'Cruz et al., 2000). Geologically, it is situated between the northern margin of the Kodaikanal charnockite massif and the southern limit of the older granulite terranes of the Nilgiri Hills, with the predominant charnockitic lithologies of the Biligirirangan Hill massif lying further north (Peucat et al., 1989). The present-day Western Ghats landscape is interpreted as the product of differential uplift during the Miocene–Pliocene, with the Palakkad Gap representing a tectonically controlled breach in the mountain chain (D'Cruz et al., 2000; Collins et al., 2007). Structurally, the gap coincides with the northern and southern extensions of the Palghat–Cauvery Shear Zone (PCSZ), a major crustal discontinuety that is considered a primary control in the development of this low-altitude corridor (Santosh et al., 2004; Ganguli et al., 2021).

The Palakkad Gap forms part of one of the oldest crustal segments within the Southern Granulite Terrain (Figure 2), comprising a diverse lithological assemblage that includes charnockite, hornblende–biotite gneiss, biotite gneiss, granitic gneiss, mylonitic augen gneiss, amphibolite, calc-alkaline intrusives, metapelites, and pegmatite bodies (Ravindrakumar & Chacko, 1994; D'Cruz et al., 2000). Petrographic and structural investigations indicate that the PCSZ imparted a strong ductile shear fabric to the region's rocks (Santosh et al., 2004; Collins et al., 2007). Pegmatite bodies in the area frequently crosscut hornblende–biotite gneiss, charnockite, and associated lithologies. Field evidence suggests that syn-intrusive pegmatites emplaced during ductile deformation were themselves deformed along with their gneissic hosts. Moreover, numerous unaltered pegmatite veins are observed to crosscut earlier pegmatites multiple times, implying a complex tectonothermal history involving repeated deformation events.

The hornblende–biotite gneiss of the Palakkad region exhibits a prominent east–west trending mineral lineation, characterized by clear evidence of dextral shearing. Shear indicators such as augen structures, pull-apart features, rootless and sheath folds, minor shear bands, and distinctive quartz fabric collectively confirm the operation of ductile dextral shear within this terrain (D'Cruz et al., 2000).

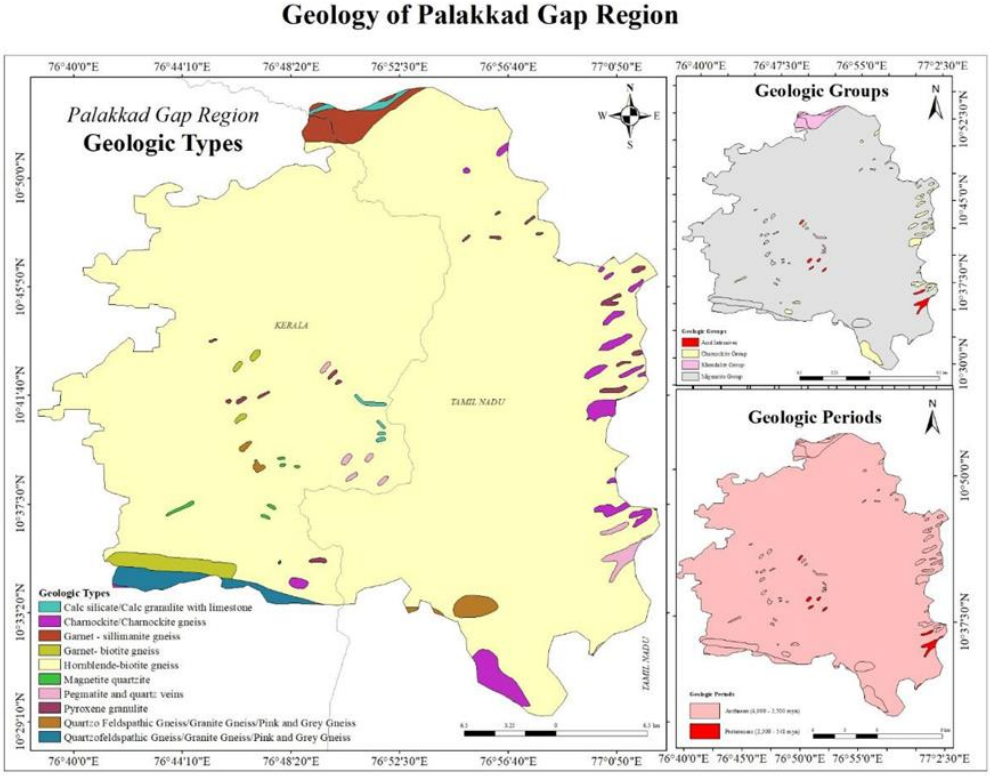

Figure 2. Geology of the Palghat Gap.
Hornblende Biotite Gneiss Covers Almost all of the Study Area

Topographic analyses of the Palakkad Gap further reveal significant linearity in the drainage network, with the gap proper hosting high-order consequent rivers, in contrast to the closely spaced, lower-order trellis, dendritic, and subsequent drainage patterns developed along the adjacent hill ranges. The geomorphic setting of the gap is marked by a well-defined low-level undulating relief (Subramanian & Muraleedharan, 1985), characterized by convex, gently graded interfluves that slope down to broad valley floors containing erosional remnants. These erosional forms are frequently inter-fingered with alluvial plains and lateritic hummocks, collectively representing a dissected pediment surface.

Geomorphologically, the study area (Figure 1) may be divided into two principal units: i) the active floodplain of fluvial origin, and ii) the pediment–peneplain complex of denudational origin, along with patches of anthropogenic terrain. The region is mantled by lateritic cover of variable thickness, classified into lateritic interfluves, dissected pediments, and valley flats, with sporadic denudational hills located in the northern and southern margins of the Palakkad Gap. The broader state of Kerala, including the Palakkad Gap, is dominated by ferruginous lateritic soils (red soils) and associated soil types. These laterites, developed under humid tropical climatic regimes, are classified into inceptisols, alfisols, mollisols, and ultisols, reflecting advanced pedogenetic processes in the region (Varghese & Byju, 1993; Sehgal, 1998; Chandran et al., 2000; Chandran et al., 2005; Bhattacharyya et al., 2009; Pal et al., 2014).

Methods and Materials

The Palakkad Gap constitutes a major physiographic break in the otherwise continuous Western Ghats, serving as a natural corridor linking Palakkad district in Kerala with Coimbatore district in Tamil Nadu. To delineate the study region, a hierarchical terrain classification approach was employed following the methodology of Chattopadhyay & Chattopadhyay (1994). The classification was based on four geomorphic parameters: slope, relative relief, drainage density, and dissection index. Areas with slopes of less than 5% were selected as part of the study region. Relative relief was defined using a threshold of 5 meters within a grid of 1 km², while drainage density greater than 1 km/km² was adopted as a criterion for hydrological characterization. The dissection index, representing surface roughness, was computed as the ratio between maximum relative relief and maximum absolute relief within each 1 km² grid cell. The integration of these four thematic layers was achieved through overlay analysis in a Geographic Information System, thereby extracting the precise extent of the study area.

A total of twenty-two surface soil samples were systematically collected from different geological units of the study area, encompassing the Palakkad and Coimbatore districts, using a grid-based soil sampling method (Figure 3). Approximately 500 g of each sample was prepared for XRD analysis to identify the mineralogical composition of the soils. The analyses were conducted at the Kerala Forest Research Institute, Peechi, Kerala, employing a Rigaku Miniflex 600 XRD instrument. This instrument, configured in vertical geometry with θ–2θ goniometer optics, operates within the angular range of −3° to 145° (2θ) and a goniometer radius of 150 mm. The scanning speed ranged between 0.01° and 100° per minute with a step size ≤ 0.005° (2θ). Mineral phases were identified by analyzing the diffraction peaks using Smart Lab Studio-II software, ensuring precise interpretation of soil mineralogy.

Thin sections of weathered rock samples were also prepared to examine mineral alteration patterns associated with weathering in the study area. Furthermore, soil series data were obtained to characterize key pedological attributes, including soil texture, mineralogy, temperature regime, reaction (pH), soil order, sub-order, great group, subgroup, and soil moisture regime. Based on these data, a soil series map was prepared to delineate the spatial variability of soils across the study region. This pedological classification was subsequently correlated with the mineralogical results obtained from XRD analysis, enabling a comprehensive interpretation of the relationship between parent material weathering, soil formation processes, and resultant mineralogical composition (cf. Sehgal, 1998; Bhattacharyya et al., 2009; Pal et al., 2014).

Figure 3. a) shows the soil collected from Kollenkode, Kerala area. b) The soil from the Pollachi, Tamil Nadu area shows a fine texture with few granules. Topsoil is removed by a steel scoop and the fresh portion of the soil is collected from this small pit c) The top portions of the soil are removed from the steel scoop and the fresh portion of soil is collected from Avalchinampalayam, Tamil Nadu area. The soil shows moisture content and is slightly reddish-black in color due to the oxidation and organic content of the soil. d) The photograph shows reddish lateritic cover soil collected in a field from Santhegoundampalayam, Tamil Nadu. e) The photograph shows the fine and coarse texture of soil at the top and the bottom of the soil profile, respectively. The top portion is slightly leached, and the bottom coarse grains show oxidized coatings in this soil profile where the soil collected from Vadakarapathy, Kerala. f) The photograph shows fine texture and moderately compacted soil due to the mixed portions of clay in the soil profile. The soil profile shows dark thick clay interbed (red pen indicates the bottom of clay bed) within the topsoil and bottom leached soil. The soil is collected from Kollengode, Kerala.

RESULT AND DISCUSSION

X-Ray diffraction

The results of the XRD analysis are presented in Table 1. The diffraction patterns display mineral peak intensities plotted as a function of the 2θ angle, with representative patterns for selected soil samples shown in Figures 4–7. The analyses revealed the presence of several key mineral feldspar, quartz, kaolinite–illite, gibbsite, goethite, calcite, vermiculite, mica, and chlorite each indicative of specific weathering environments. Among these, feldspar and quartz were the most consistently detected, occurring in nearly all samples except for sample 1032 from Valara, in which feldspar was absent. Quartz, owing to its remarkable resistance to chemical weathering, was generally observed in concentrations comparable to or slightly lower than feldspar. Feldspar, though relatively resistant, undergoes hydrolysis under favourable conditions, releasing ions that ultimately form clay minerals such as gibbsite.

The dominance of feldspar and quartz across the study area reflects the felsic mineral-rich nature of the underlying parent rocks, which predominantly include hornblende–biotite gneiss and charnockitic gneiss, intruded locally by granite, pegmatite, and quartz veins. Globally, feldspar and quartz are among the most widespread soil-forming minerals, generated through the mechanical and chemical disintegration of rock masses under the influence of gravity, slope gradient, and

hydrological processes. During progressive weathering, soluble ions are leached away while residual minerals accumulate in situ, modifying soil texture and structure. As summarized in Table 2, feldspar and quartz alternate as the most abundant first- and second-ranked minerals across samples, while quartz consistently displays higher resistance to weathering compared to feldspar. In the diffraction patterns, feldspar exhibited distinct peaks at 13.6° and 27.12–28.48° (2θ), whereas quartz displayed a dominant peak at 26.58–26.76° (2θ). Weathering of feldspar is associated with the formation of kaolinite (Fernández-Caliani et al., 2010), illite (Bétard et al., 2009), and mixed-layer clays (Wang et al., 2012).

Alongside feldspar and quartz, gibbsite was identified as a significant secondary mineral in nearly all samples. The occurrence of gibbsite is particularly note-worthy, as its slow rate of formation implies relatively old soils, while its abundance is typically enhanced in humid tropical climates where intense hydrolysis and leaching dominate (Wang et al., 1981; Ogg & Baker, 1999). The presence of gibbsite in the studied soils may therefore indicate long-term pedogenesis under high-temperature and high-rainfall conditions. Kaolinite–illite also appeared in most samples at appreciable concentrations, while minerals such as goethite, calcite, vermiculite, mica, and chlorite were identified sporadically. The oxide minerals particularly goethite, gibbsite, and hematite are closely associated with advanced weathering regimes marked by high rainfall and intense desilication (Van der Merwe & Weber, 1963). Within the diffraction spectra, gibbsite exhibited characteristic peaks between 20.81° and 20.98° (2θ), further confirming its signi-ficant presence in the soils of the Palakkad Gap.

Gibbsite $Al(OH)_3$ is a secondary insoluble mineral formed through the hydrolytic weathering of alumino-silicate minerals, wherein aluminum is leached from parent phases such as biotite and feldspar and subsequently re-precipitated as gibbsite. It represents one of the most common aluminum oxide minerals and is a principal constituent of lateritic soils and bauxitic crusts. Gibbsite is typically generated by the direct weathering of Al-hydroxide–bearing minerals, including orthoclase, feldspar, and biotite, which are abundantly present in the pegmatitic intrusions, feldspathic hosts, and gneissic rocks of the Palakkad Gap region (Bhattacharyya et al., 2000).

The mineral may also form through the progressive desilication of kaolinite or halloysite, particularly in granite- and volcanic-derived soils, as earlier documented by Bates (1971) and Tazaki (1976). Its occurrence is strongly associated with tropical climates, where high rainfall and elevated temperatures accelerate leaching, hydrolysis, and the development of thick weathering profiles. Within such environments, gibbsite is widely distributed throughout soil profiles as part of lateritic and bauxitic horizons, commonly forming weathering crusts. Importantly, gibbsite exhibits relatively slow rates of alteration compared to other secondary minerals, and its persistence in the study area suggests advanced and progressive stages of weathering under warm, humid tropical conditions.

Microprobe mineral analyses confirm that gibbsite may form through the progressive weathering of biotite, with intermediate transformation to kaolinite before crystallizing into gibbsite, as demonstrated by Jolicoeur et al. (2000). Scanning electron microscopy (SEM) investigations by Chandran et al. (2005) further revealed broken gibbsite crystals along with dissolution features and etch pits developed within feldspar grains, suggesting that direct feldspar-to-gibbsite transformation is also a widespread pedogenic pathway (Chandran et al., 2005). Additional SEM studies on highly acidic Ultisols derived from red ferruginous soils of Kerala's humid tropical environment confirmed the presence of well-developed gibbsite crystals, emphasizing the advanced degree of weathering under such conditions (Balasubramaniam & Sabale, 1984; Pal et al., 2014).

Although gibbsite is typically associated with alkaline environments, where its stability is favoured (Tait et al., 1983; Balasubramaniam & Sabale, 1984), the occurrence of gibbsite in acidic soils of Kerala highlights an unusual geochemical setting. This anomaly underscores the intensity of tropical weathering and desilication processes, which are capable of producing and stabilizing gibbsite even in acidic soil regimes (Pal et al., 2014).

Table 1. The Minerals Present in the Samples Analyzed by X-ray Diffraction

S. No	Sample	Sample Locations	Fsp	Qtz	Gib	K-ill	Goe	Mica	Ver	Cal	Chl
1	PGT 37	Mullakkal Challa	×	×	×	-	×	-	×	×	-
2	PGT 112	Parayampallam	×	×	×	×	-	-	-	-	-
3	PGT 140	Gopalapuram	×	×	×	×	-	-	-	-	-
4	PGT 168	Chinganchira	×	×	×	×	×	-	-	-	-
5	PGT 262	Avalchinnam	×	×	×	-	×	-	-	-	-
6	PGT 455	Nanjengoundar Pudur	×	×	×	×	-	-	×	-	-
7	PGT 498	Vilayodi	×	×	×	×	-	-	-	-	-
8	PGT 740	Nattupathy	×	×	×	×	-	-	-	-	-
9	PGT 796	Aachipatti	×	×	×	×	×	-	-	-	-
10	PGT 799	Nerukukkad, Verkoli	×	×	×	-	-	-	-	-	-
11	PGT 840	Malankkat	×	×	×	×	-	-	-	-	-
12	PGT 876	Pothanaikkan Challa	×	×	×	×	-	-	-	-	-
13	PGT 881	Rangasamudram	×	×	×	×	-	×	-	-	-
14	PGT 884	Ayyanpathy	×	×	×	×	-	×	-	-	-
15	PGT 884A	Ayyanpathy	×	×	×	-	-	×	-	-	-
16	PGT 920	Kamblichungam	×	×	×	-	-	-	-	-	-
17	PGT 984	Kunjuvallampathy	×	×	×	×	×	-	-	-	-
18	PGT 1016	Nellimedu	×	×	×	×	-	-	-	-	-
19	PGT 1032	Valara	-	×	×	×	-	×	-	-	-
20	PGT 1050	Chemmanapathy	×	×	×	×	-	-	-	-	-
21	PGT 1210	Vadakkipalayam	×	×	×	×	-	-	-	-	×
22	PGT 1251	Vadakarapathy	×	×	×	×	-	-	-	-	-

Note: ×=Mineral present; -=Mineral not present
Fsp=Feldspar; Qtz=Quartz; Gib=Gibbsite; K-ill=Kaolinite-illite; Goe=Goethite; Ver=Vermiculite; Cal=calcite; Chl=Chlorite.

Table 2. Dominance Ranking of Soil Minerals in Percentage

S. No	Sample	1st Rank		2nd Rank		3rd Rank		4th Rank	
		Mineral	%	Mineral	%	Mineral	%	Mineral	%
1	PGT 37	Qtz	34.75	Fsp	30.27	Gib	17.25	Cal	9
2	PGT 112	Qtz	42.96	Fsp	31.64	Gib	24.30	Kao-ill	1.10
3	PGT 140	Fsp	47.67	Qtz	29.07	Gib	19.11	Kao-ill	4.14
4	PGT 168	Fsp	50.75	Qtz	20.92	Gib	15.94	Goe	11.38
5	PGT 262	Qtz	79.13	Fsp	14.76	Gib	4.12	Goe	1.98
6	PGT 455	Fsp	57.24	Qtz	15.16	Ver	12.41	Kao-ill	10.44
7	PGT 498	Qtz	38.22	Fsp	33.05	Gib	26.18	Kao-ill	2.55
8	PGT 740	Fsp	40.25	Qtz	32.42	Gib	22.16	Kao-ill	-
9	PGT 796	Fsp	46.67	Qtz	19.14	Goe	13.93	Kao-ill	10.53
10	PGT 799	Qtz	59.51	Fsp	21.92	Gib	18.57	-	-
11	PGT 840	Qtz	49.8	Fsp	28.60	Gib	15.40	Kao-ill	6.30
12	PGT 876	Fsp	59.97	Qtz	18.97	Gib	17.10	Kao-ill	3.96
13	PGT 881	Fsp	60.14	Qtz	21.76	Gib	13.16	Mica	3.38
14	PGT 884 A	Fsp	54.28	Mica	10.67	Gib	10.67	Qtz	10.67
15	PGT 884	Qtz	32.12	Fsp	25.55	Gib	24.18	Mica	14.55
16	PGT 920	Qtz	60.98	Gib	22.32	Fsp	16.70	-	-
17	PGT 984	Fsp	60.97	Qtz	17.43	Gib	17.13	Goe	2.97
18	PGT 1016	Fsp	56.29	Qtz	23.92	Kao-ill	9.99	Gib	9.79
19	PGT 1032	Kao-ill	99.99	Qtz	00.01	Gib	0.0023	Mica	0.0003
20	PGT 1050	Fsp	52.67	Qtz	27.82	Gib	16.86	Kao-ill	2.65
21	PGT 1210	Fsp	52.67	Qtz	18.27	Gib	17.97	Kao-ill	4.71
22	PGT 1251	Fsp	64.96	Qtz	23.54	Gib	10.56	Kao-ill	0.94

Note: Qtz=Quartz; Fsp=Feldspar; Gib=Gibbsite; Kao-ill=Kaolinite-illite; Ver=Vermiculite; Goe=Goethite; Cal=calcite.
The feldspar and quartz minerals interchangeably present as first and second-ranking minerals. The gibbsite and kaolinite present as third and fourth-ranking minerals in the XRD analysis.

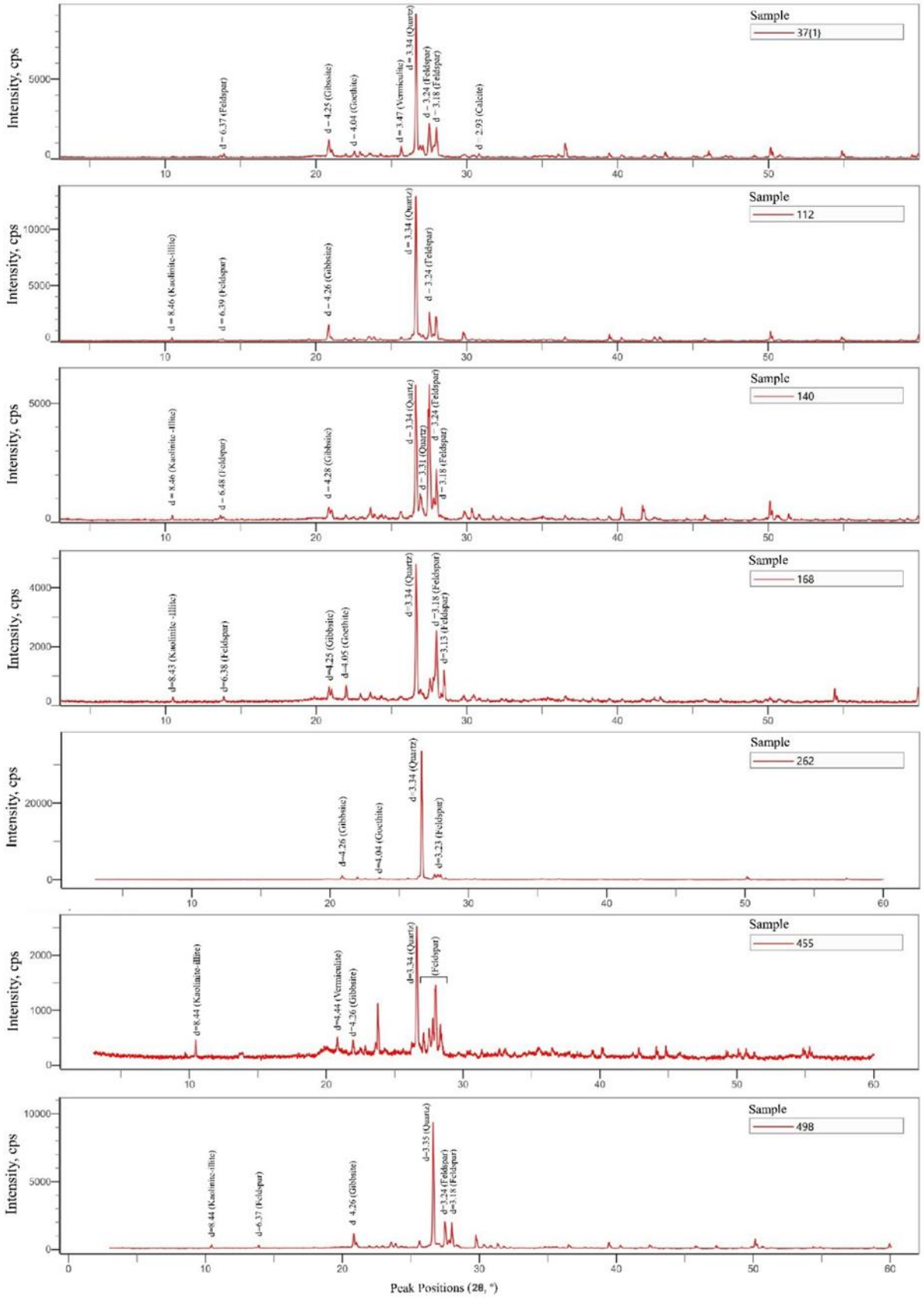

Figure 4. X-ray Diffraction Pattern of Respective Mineral Peaks of Soil Samples 37, 112, 140, 168, 262, 455, and 498. The Pattern Shows the Peak Position Values in 2θ° and The Intensity of the Mineral in Counts Per Second

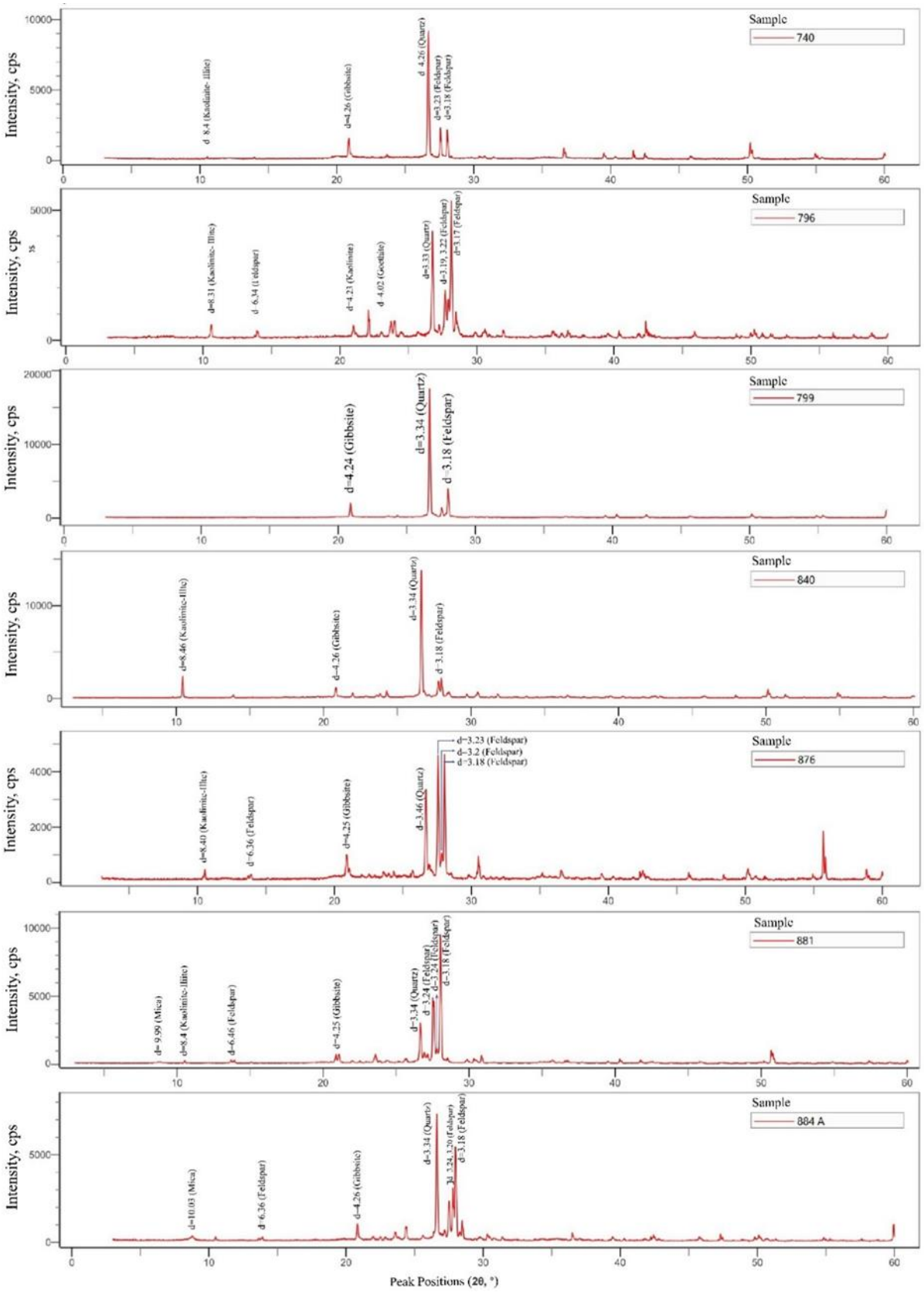

Figure 5. X-ray Diffraction Pattern of Respective Mineral Peaks of Soil Samples 740,796,799, 840, 876, 881, and 884A. The Pattern Shows the Peak Position Values in 2θ° and the Intensity of the Mineral in Counts Per Second

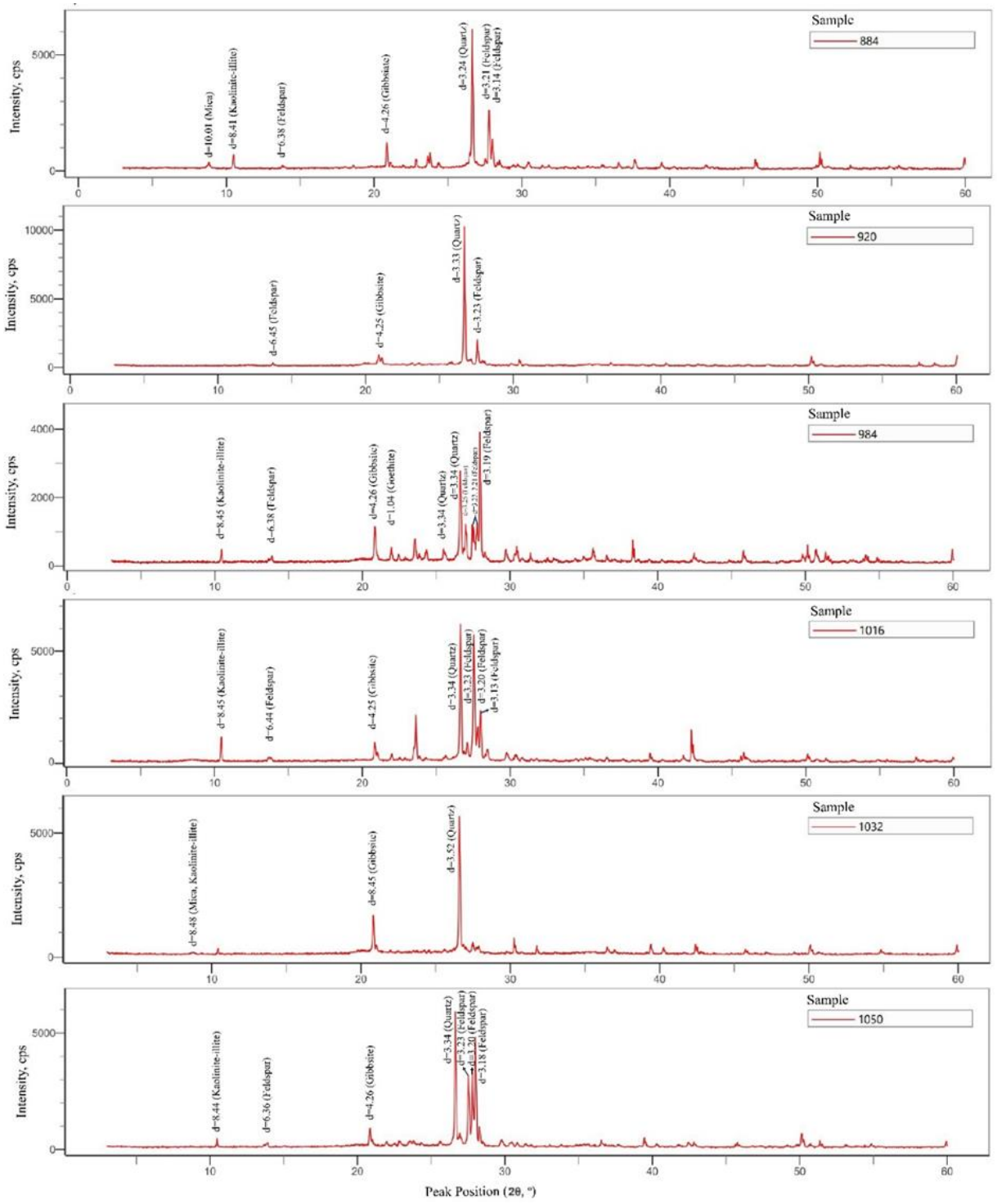

Figure 6. X-ray Diffraction Pattern of Respective Mineral Peaks of Soil Samples 884, 920, 984, 1016, 1032, and 1050. The Pattern Shows the Peak Position Values in 2θ° and the Intensity of the Mineral in Counts Per Second

The pH diagram (Figure 8) indicates that gibbsite formation occurs during the early stages of soil development, typically under slightly alkaline to neutral conditions. The study area is underlain predominantly by hornblende–biotite gneiss with pegmatitic intrusions, where the abundance of feldspar and biotite provides a primary source of aluminum. During incipient weathering, these minerals undergo hydrolysis and desilication, resulting in the crystallization of gibbsite within the soil profile.

In addition to gibbsite, kaolinite

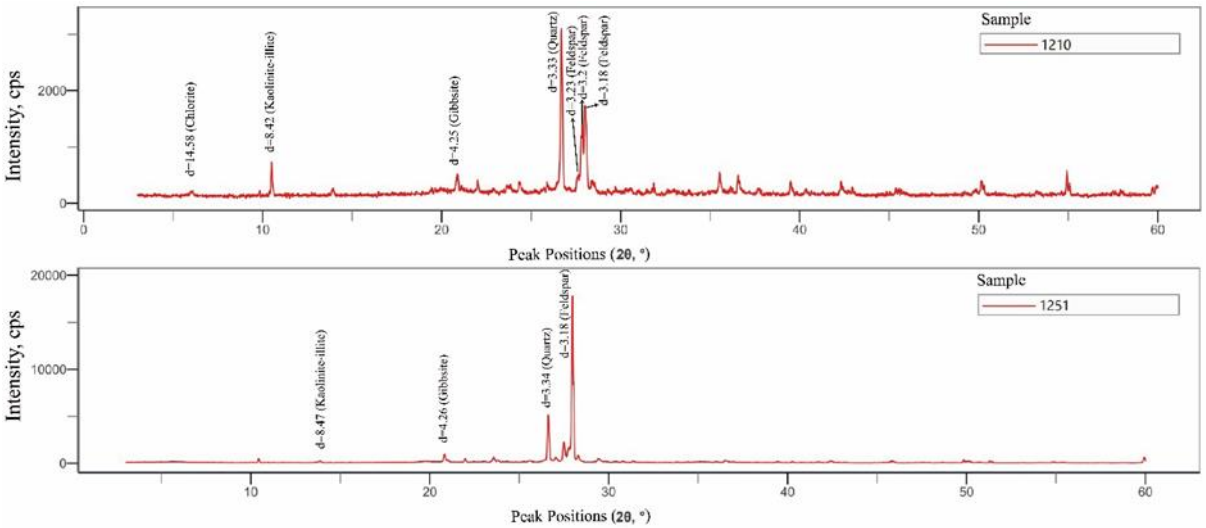

Figure 7. X-ray Diffraction Pattern of Respective Mineral Peaks of Soil Samples 1210 and 1251. The Pattern Shows the Peak Position Values in 2θ° and the Intensity of the Mineral in Counts Per Second.

$Al_2Si_2O_5(OH)_4$, a hydrous aluminum silicate, was also identified in significant concentrations in the soils of the Palakkad Gap. The XRD analysis revealed characteristic kaolinite peaks between 10.42° and 10.6° (2θ). Kaolinite is widely recognized as a dominant mineral in the humid tropical soils of Kerala and Tamil Nadu, particularly within Alfisols and Ultisols (Bhattacharyya et al., 2009). According to Aleva (1983), kaolinite and gibbsite represent the most common and stable end-products of prolonged chemical weathering in humid tropical environments.

Kaolinite is generally abundant in Oxisols and is formed through kaolinization processes, either by the direct alteration of feldspar or through the pseudomorphic alteration of biotite. In the Palakkad Gap, the occurrence of kaolinite–illite assemblages most likely reflects the intermediate stages of feldspar leaching under humid tropical climatic conditions. These processes are consistent with the pedogenic evolution of soils across multiple taxonomic groups, including Inceptisols, Entisols, Alfisols, and Ultisols, all of which are represented within the study area.

The XRD analysis identified several secondary minerals in the soils of the Palakkad Gap. Goethite was detected at peaks between 21.94° and 22.07° (2θ). Goethite (FeOOH), an iron oxide mineral, is a thermodynamically stable and widespread pedogenic product, commonly occurring in ores, sediments, and soils (Cornell & Schwertmann, 2003; Liu et al., 2014). It is typically derived from the weathering of iron-bearing rocks such as biotite, magnetite, ilmenite, pyrite, hornblende, and pyroxenes (Kemp, 1985), all of which are well-represented in the lithology of the study area. Goethite was identified in five of the analyzed soil samples. The presence of kaolinite–gibbsite–goethite assemblages is characteristic of strongly weathered profiles in high-rainfall zones of the Western Ghats, where intense chemical weathering promotes residual accumulation of these minerals (Deepthy & Balakrishnan, 2005).

Vermiculite, a hydrated magnesium–aluminum–iron silicate, was also detected in the soils, with XRD peaks occurring between 19.83° and 25.63° (2θ). Vermiculite commonly represents an early alteration product of mica group minerals (muscovite, biotite) and chlorite (Potter, 2000; Wang et al., 2017), and its formation is generally favored in environments receiving annual precipitation greater than 100 cm (Barshad, 1966). Among the samples, vermiculite was identified only in two locations are Mullakkal Challa (PGT 37) and Nanjengoundar Pudur (PGT 455), likely reflecting localized alteration of biotite-rich parent material.

Calcite ($CaCO_3$) was detected only in the Mullakkal Challa (PGT 37) sample, constituting approximately 9% of the mineral composition, with XRD peaks at 29.81°, 30.45°, and 30.81° (2θ). Calcite typically accumulates in soils through two mechanisms: i) precipitation from soil water enriched with dissolved calcium ions, and ii) direct

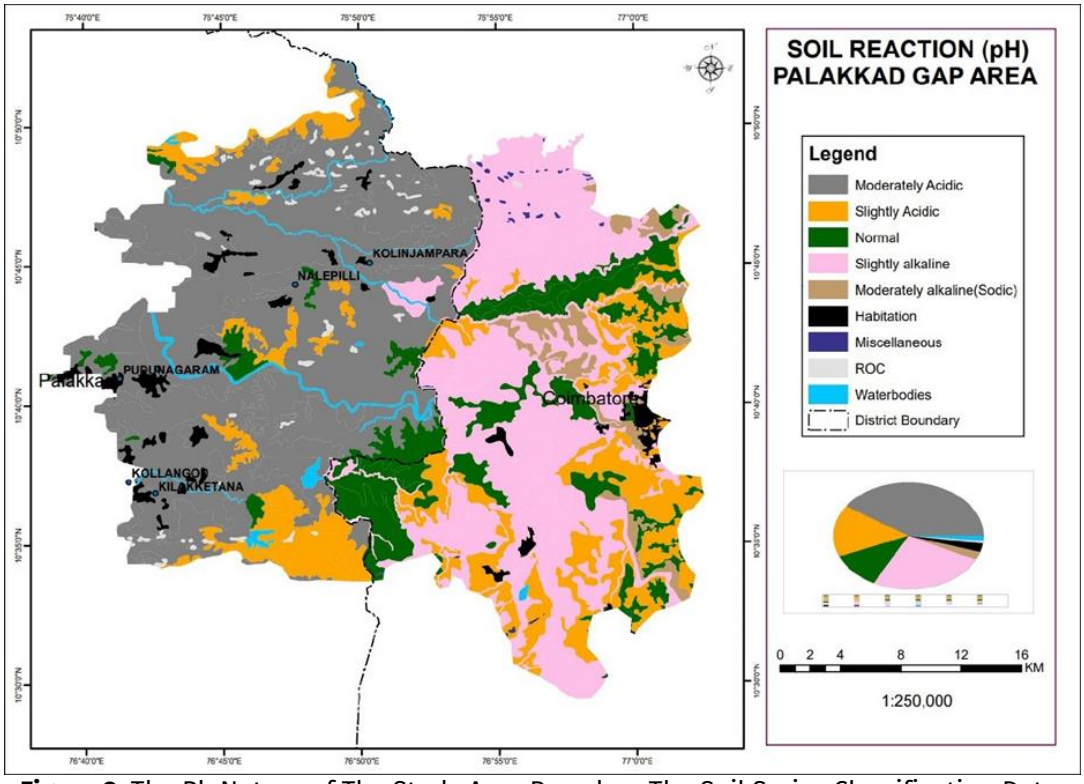

Figure 8. The Ph Nature of The Study Area Based on The Soil Series Classification Data. The Eastern Part of The Study Area is Slightly Alkaline in Condition, and The Western Part of The Study Area is Moderately Acidic. The Study Area as A Whole is Slightly Acidic to Neutral

atmospheric deposition of calcium-bearing particles, facilitated by elevated soil pH and higher CO_2 partial pressures in the vadose zone (Liu & Dreybrodt, 1997; Lal, 2008).

Calcite occurrence in the Palakkad Gap is rare. The soils are moderately acidic to neutral, with slightly alkaline patches (Figure 8), conditions that generally inhibit calcite stability. Moreover, the absence of calcite-bearing parent rocks and the dominance of acidic soil series further restrict calcium carbonate accumulation. Where deposited, calcite is readily dissolved under acidic conditions, preventing long-term buildup in the soil profile.

Finally, the electrical conductivity (EC) analysis confirms the non-saline character of the study area (Figure 9). This reinforces the interpretation that the Palakkad Gap soils, despite localized calcite presence, are not sites of significant carbonate accumulation due to the prevailing moderately acidic to slightly alkaline pedochemical environment.

The soils in the study area have values consistently falling within the range of EC < 2 dS m^{-1}, corresponding to the non-saline class (Richards, 1954). This observation suggests that soluble salt accumulation is negligible, a condition also supported by the limited occurrence of calc-alkaline intrusive lithologies in the region.

Among secondary minerals, chlorite a relatively stable mineral commonly found in the clay fractions of soils worldwide (Brady & Weil, 2008) was largely absent in the studied soils. Only one location, Vadakkipalayam Pirivu in Tamil Nadu, contained detectable chlorite, amounting to 2.20% of the whole mineral assemblage, with its characteristic XRD peak observed at 6.09° (2θ).

Similarly, mica minerals were sparsely represented in the soils. Out of the total samples analyzed, mica was detected in only four samples from three locations: Rangasamudram, Ayyanpathy, and Valara. The presence of mica was confirmed by XRD peaks between 8.76° and 8.86° (2θ). These occurrences suggest that while remnants of primary phyllosilicates persist in localized pockets, they are generally unstable under the prevailing humid tropical weathering regime of the Palakkad Gap, which favors their progressive alteration into secondary clay minerals such as kaolinite and vermiculite (Pal et al., 2014; Bétard et al., 2009).

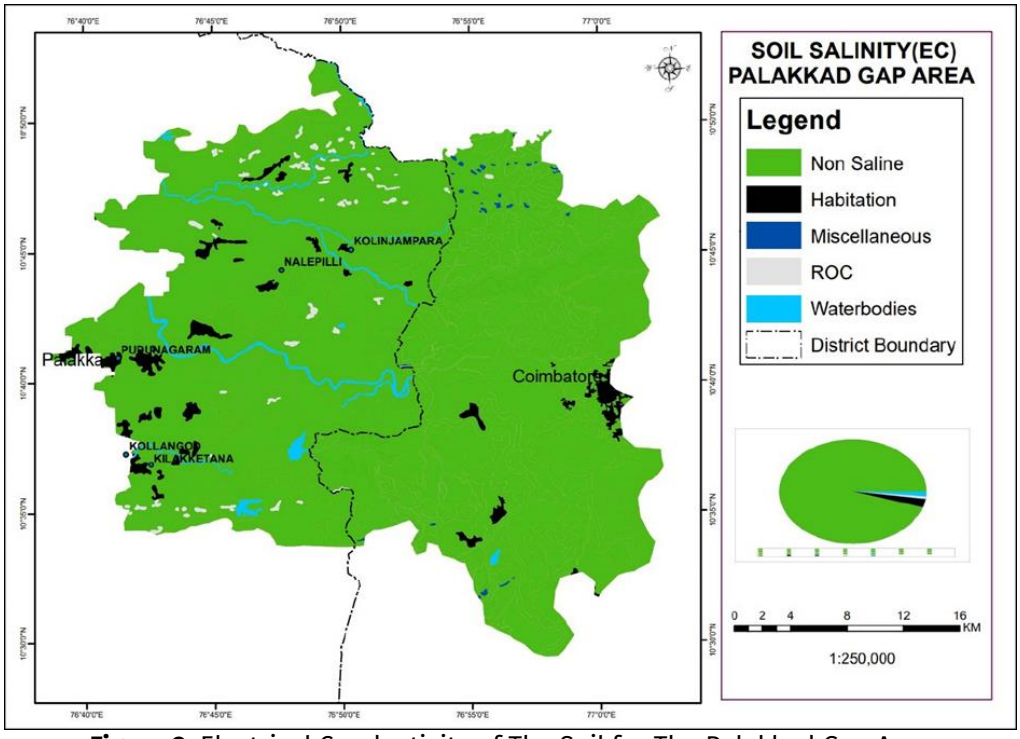

Figure 9. Electrical Conductivity of The Soil for The Palakkad Gap Area It Shows Almost All of The Study Area is Non-Saline (EC = 0 < 2) Based on The Salinity Class.

Petrography

The lithology of the study area is primarily composed of hornblende–biotite gneiss, quartzofeldspathic gneiss, biotite gneiss, and charnockite. For petrographic investigation, weathered samples of quartzofeldspathic gneiss and hornblende–biotite gneiss were collected from representative localities within the region. Thin-section analysis of these samples reveals incipient stages of chemical weathering, characterized by the alteration of mineral grain boundaries to Fe-oxide phases and the development of secondary alteration products from specific primary minerals (cf. Velmurugan et al., 2016).

Soil Series Classification

The soil series analysis (Table 3) reveals that the Palakkad Gap hosts a diverse assemblage of soil orders, including Inceptisols, Entisols, Alfisols, and Ultisols, arranged in decreasing order of dominance. Using the soil series data, a spatial distribution map was prepared (Figure 10) to illustrate the geographic extent of these soil orders across the study area. Among them, Inceptisols constitute the predominant soil order, reflecting the relatively young and weakly developed pedogenic profiles typical of landscapes undergoing active geomorphic processes (Soil Survey Staff, 2014).

Texturally, the soils are classified as fine, fine-loamy to clayey-skeletal, with a mixed mineralogical composition dominated by clay-structured mineral assemblages. These soils have developed under a hyperthermic soil temperature regime, consistent with the humid tropical climatic conditions of Kerala and Tamil Nadu (Sehgal, 1998; Pal et al., 2014). The soils exhibit both calcareous and non-calcareous variants; however, non-calcareous soils are more widespread, suggesting limited carbonate accumulation under the prevailing moderately acidic to neutral pedochemical environment.

The soil series data indicate that the soils of the Palakkad Gap exhibit a moderately acidic to slightly alkaline pH range, reflecting variable pedochemical conditions across the region. Bhattacharyya et al. (2009) documented that under humid tropical conditions in Kerala, soil orders such as Inceptisols, Alfisols, Mollisols, and Ultisols are widespread, shaped by parent material and climatic controls. Within the study area, Inceptisols and Entisols dominate, with localized occurrences of Alfisols and Ultisols. These latter soil orders are commonly associated with secondary minerals such as gibbsite and kaolinite, which require specific temperature and moisture regimes for their stability and are considered characteristic products of prolonged weathering in humid

Table 3. Soil Series Classification for Palghat Gap Region

Soil Series	pH	EC	Textural Class	Mineralogy	Temperature Regime	Soil Reaction	Soil Classification	Order	Sub Order	Great Group	Subgroup
Alagapuri	6.1	0.20	Fine	MM*	Isohyperthermic	Calcareous	Vertic Haplustepts	Inceptisols	Ustepts	Haplustepts	Vertic
Anakkal	5.5	0.25	Clayey skeletal	Mixed	Isohyperthermic	Non-calcareous	Typic Hapludults	Ultisols	Aquults	Hapludults	Typic
Anamalai	6.3	0.77	Fine loamy	Mixed	Isohyperthermic	Non-calcareous	Fluventic Haplustepts	Inceptisols	Ustepts	Haplustepts	Fluventic
Annur	7.6	0.18	loamy skeletal	Mixed	Isohyperthermic	Non-calcareous	Lithic Rhodustalfs	Alfisols	Ustalfs	Rhodustalfs	Lithic
Attipalayam	7.9	0.18	Fine	Mont	Isohyperthermic	Calcareous	Vertic Haplustepts	Inceptisols	Ustepts	Haplustepts	Vertic
Chuduvalattur	5.4	0.08	Fine loamy	Mixed	Isohyperthermic	Non-calcareous	Typic Hapludults	Ultisols	Aquults	Hapludults	Typic
Chullimada	6.1	0.05	loamy skeletal	Mixed	Isohyperthermic	Non-calcareous	Typic Udorthents	Entisols	Orthents	Udorthents	Typic
Dasarapatti	8.0	0.82	Fine	Mont	Isohyperthermic	Calcareous	Gypsic Haplustepts	Inceptisols	Ustepts	Haplustepts	Gypsic
Ilayaimuthur	7.9	0.30	clayey skeletal	Mixed	Isohyperthermic	Non-calcareous	Lithic Haplustepts	Inceptisols	Ustepts	Haplustepts	Lithic
Irugur	8.0	0.26	Fine loamy	Mixed	Isohyperthermic	Non-calcareous	Typic Haplustepts	Inceptisols	Ustepts	Haplustepts	Typic
Kalkalam	5.2	0.20	Fine loamy	Mixed	Isohyperthermic	Non-calcareous	Typic Udipsamments	Entisols	Psamments	Udipsamments	Typic
Kallivalasu	8.2	0.30	Fine loamy	Mixed	Isohyperthermic	Calcareous	Fluventic Haplustepts	Inceptisols	Ustepts	Haplustepts	Fluventic
Kanjampatti	7.6	0.08	Fine loamy	Mixed	Isohyperthermic	Non-calcareous	Typic Haplustepts	Inceptisols	Ustepts	Haplustepts	Typic
Kattampatti	8.4	0.55	Fine	Mont	Isohyperthermic	Calcareous	Vertic Ustorthents	Entisols	Orthents	Ustorthents	Vertic
Kumbamala	5.9	0.08	loamy	Mixed	Isohyperthermic	Non-calcareous	Typic Udorthents	Entisols	Orthents	Udorthents	Typic
Kundur	6.6	0.05	Fine loamy	Mixed	Isohyperthermic	Non-calcareous	Typic Dystrudepts	Inceptisols	Udepts	Dystrudepts	Typic
Kunnathur	6.7	0.25	clayey skeletal	Mixed	Isohyperthermic	Non-calcareous	Lithic Rhodustalfs	Alfisols	Ustalfs	Rhodustalfs	Lithic
Kunpulli	5.7	0.04	Fine loamy	Mixed	Isohyperthermic	Non-calcareous	Typic Dystrudepts	Inceptisols	Udepts	Dystrudepts	Typic
Malampuzha	5.9	0.13	coarse loamy	Mixed	Isohyperthermic	Non-calcareous	Typic Udipsamments	Entisols	Psamments	Udipsamments	Typic
Mandur	5.7	0.06	Fine	Mixed	Isohyperthermic	Non-calcareous	Ruptic Alfic Dystrudepts	Inceptisols	Udepts	Dystrudepts	Ruptic Alfic
Mannur	5.2	0.06	Fine	Mixed	Isohyperthermic	Non-calcareous	Typic Dystrudepts	Inceptisols	Udepts	Dystrudepts	Typic
Mettupalaiyam	7.7	0.70	Fine	Mixed	Isohyperthermic	Non-calcareous	Rhodic Paleustalfs	Alfisols	Ustalfs	Paleustalfs	Rhodic
Muppamkulam	5.6	0.09	Fine	Mixed	Isohyperthermic	Non-calcareous	Oxic Dystrudepts	Inceptisols	Udepts	Dystrudepts	Oxic
Palathurai	8.1	0.13	Fine loamy	Mixed	Isohyperthermic	Calcareous	Typic Haplustepts	Inceptisols	Ustepts	Haplustepts	Typic
Peringottukurussi	5.3	0.05	Fine loamy	Mixed	Isohyperthermic	Non-calcareous	Aquic Dystrudepts	Inceptisols	Udepts	Dystrudepts	Aquic
Pichanur	6.9	0.12	Fine loamy	Mixed	Isohyperthermic	Non-calcareous	Typic Udipsamments	Entisols	Psamments	Udipsamments	Typic
Pilamedu	8.6	0.20	Fine loamy	Mixed	Isohyperthermic	Non-calcareous	Ultic Haplustepts	Inceptisols	Ustepts	Haplustepts	Ultic
Pudur	7.9	0.45	Fine	Mont	Isohyperthermic	Non-calcareous	Typic Haplustepts	Inceptisols	Ustepts	Haplustepts	Typic
Salaiyur	8.3	0.19	loamy skeletal	Mixed	Isohyperthermic	Calcareous	Fluventic Haplustepts	Inceptisols	Ustepts	Haplustepts	Fluventic
Somayyanur	8.2	0.20	Fine loamy	Mixed	Isohyperthermic	Non-calcareous	Typic Haplustepts	Inceptisols	Ustepts	Haplustepts	Typic
Valipparamlat	6.3	0.10	Fine loamy	Mixed	Isohyperthermic	Non-calcareous	Typic Dystrudepts	Inceptisols	Udepts	Dystrudepts	Typic
Varapatti	8.5	1.40	Fine	Mont	Isohyperthermic	Calcareous	Vertic Ustorthents	Entisols	Orthents	Ustorthents	Vertic
Velladikunnu	5.1	0.03	Fine	Mixed	Isohyperthermic	Non-calcareous	Typic Dystrudepts	Inceptisols	Udepts	Dystrudepts	Typic

Note: MM*=Mixed Montmorillonitic; Mont=Montmorillonitic

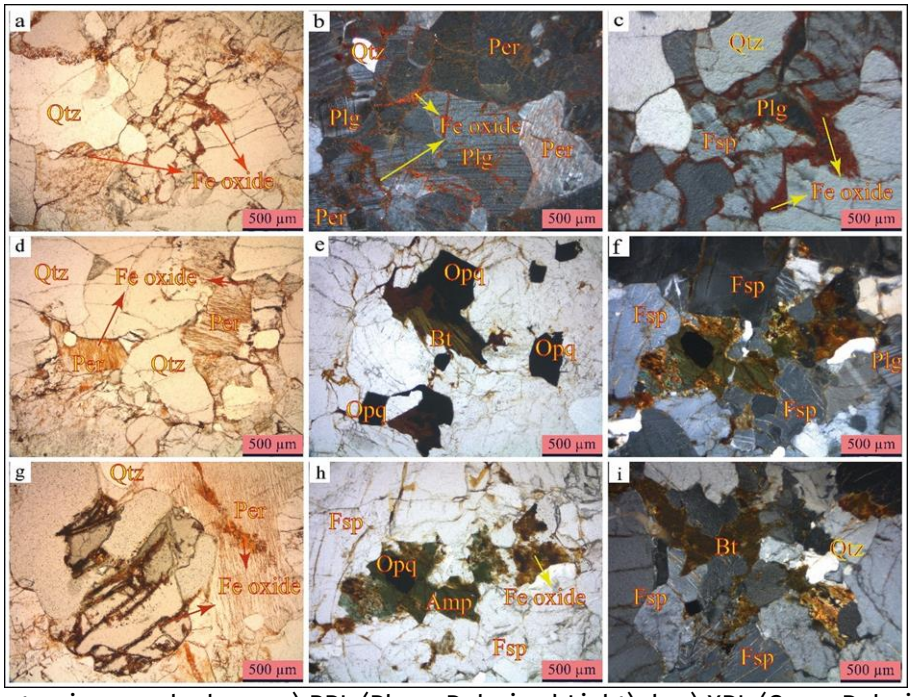

Figure 10. Photomicrograph shows a) PPL (Plane Polarized Light); b-c) XPL (Cross Polarized Light) of quartzo-feldspathic gneiss rocks show that the mineral edges of feldspar (FSP), plagioclase (Plg), quartz (Qtz), and the intermineral, intramineral fractures are occupied by Fe-oxides weathered from the accessory mafic minerals which contain Fe members; d) The photomicrograph shows that the perthite (Per) mineral cleavages are occupied by iron oxides due to the weathering process; e), g)-h) Photomicrograph of PPL shows the mafic minerals (amphibole, biotite) are altered to Fe oxide due to the weathering process; f) and i) Photomicrograph of XPL shows that mineral fractures of feldspar and mafic mineral edges are altered, and the opaque mineral magnetite weathered to Fe-oxide, which occupies the cleavages and fracture gaps.

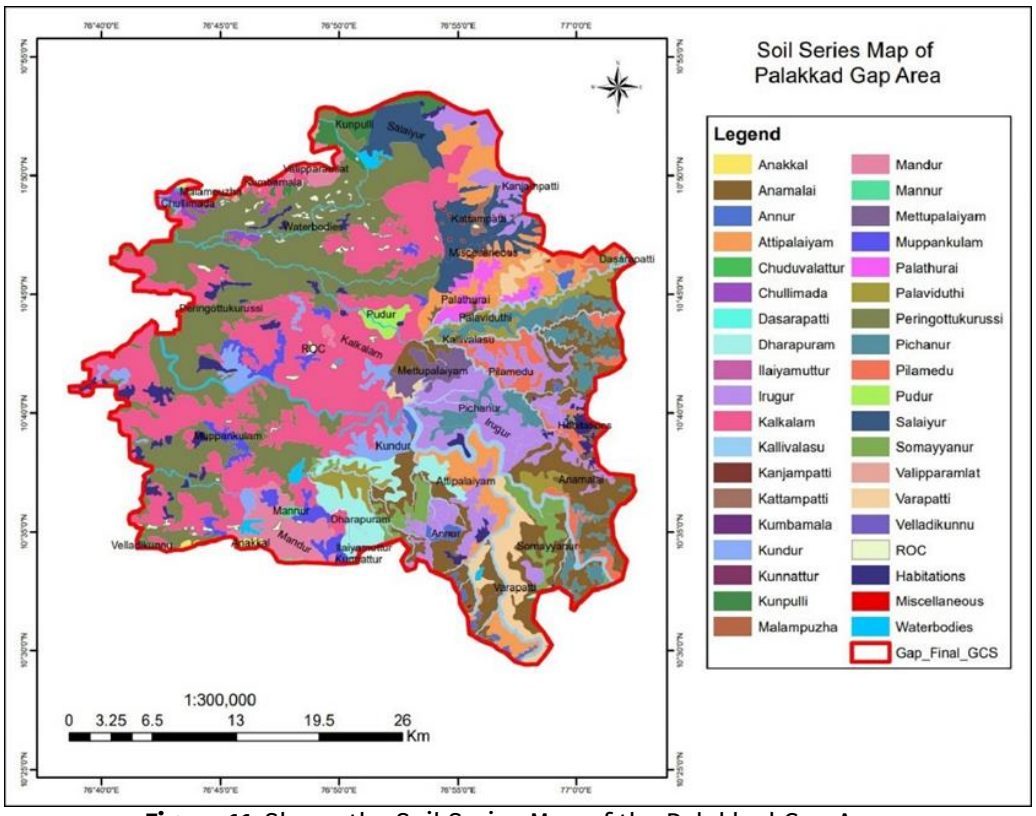

Figure 11. Shows the Soil Series Map of the Palakkad Gap Area

tropical climates. The presence of these minerals and soil orders reinforces the strong climatic control on pedogenesis in the Palakkad Gap. Regionally, the Western Ghats of Kerala, together with adjoining tracts of Tamil Nadu, host a broad spectrum of soil orders, including Inceptisols, Entisols, Alfisols, Ultisols, and Mollisols. These soils have developed on diverse parent lithologies such as gneissic complexes, granitic and ferruginous gneiss, calcareous sandstones, and basaltic terrains, under hot humid to per-humid agro-ecological regimes (Kharche, 1996; Natarajan et al., 1997; Sehgal, 1998; Shiva Prasad et al., 1998; Harindranath et al., 1999; Bhattacharyya et al., 2009; Pal et al., 2014). In the uplands of Tamil Nadu, Alfisols, Inceptisols, Ultisols, and Mollisols predominate over granitic and gneissic terrains, highlighting the role of lithology in soil differentiation. Similarly, in the Palakkad Gap, the soils have developed on gneissic, charnockitic, and granitic terrains, producing comparable soil orders. The mineralogical assemblages observed, particularly kaolinite and gibbsite, are consistent with those formed under humid tropical climatic regimes across southern India.

CONCLUSION

The east–west orientation of the Palakkad Gap exerts a strong influence on regional precipitation and atmospheric circulation, creating dynamic weathering conditions that promote the formation of soils enriched in secondary minerals. The lithological framework of the study area is dominated by hornblende–biotite gneiss, charnockite, and charnockitic gneiss, with pegmatite and quartz vein intrusions exposed along the northern and southern margins. These rocks, particularly hornblende–biotite gneiss and charnockitic gneiss, are relatively susceptible to weathering and erosion under the prevailing topographic and climatic conditions, where steep slopes and high rainfall have facilitated the development of thick lateritic covers over the Proterozoic basement (Subramanian & Muraleedharan, 1985; D'Cruz et al., 2000). Structurally, these rocks display east–west lineations consistent with the Palghat–Cauvery Shear Zone, and slope gently from east to west across the gap.

Mineralogical analyses of soil samples from the gap, based on XRD, reveal the dominance of primary minerals such as quartz and feldspar, with secondary alteration products including gibbsite and kaolinite–illite. Gibbsite and kaolinite–illite occur as third- and fourth-ranked minerals, respectively, indicating their derivation from the alteration of feldspar and biotite within the hornblende–biotite gneiss and charnockitic gneiss. Pedogenetically, gibbsite formation is favored during the early stages of weathering in slightly alkaline environments, whereas kaolinite–illite assemblages typically develop under moderately acidic to neutral conditions (Aleva, 1983; Bhattacharyya et al., 2009; Pal et al., 2014). Comparable mineral assemblages have been reported from Alfisols and Ultisols in Kerala and Tamil Nadu, highlighting the role of humid tropical climates in controlling soil mineralogy (Sehgal, 1998; Chandran et al., 2005). The near absence of calcite in most samples suggests either the dominance of acidic soil conditions or the lack of calcite-bearing lithologies in the region (Lal, 2008).

Petrographic examination of weathered rock samples further demonstrates the initial stages of soil development, with Fe-oxide precipitation along mineral cleavages and fractures and the progressive alteration of mafic minerals. These features signify incipient chemical weathering processes responsible for the breakdown of the crystalline basement into soil. In addition, the presence of indicator minerals such as goethite, mica, vermiculite, and chlorite further reflects the intensity of weathering and the pedo-environmental conditions prevailing in the gap (Potter, 2000; Cornell & Schwertmann, 2003; Wang et al., 2017).

Finally, the soil series classification of the study area confirms the presence of multiple soil orders, predominantly Inceptisols and Entisols, with localized occurrences of Alfisols and Ultisols. This diversity of soil orders underscores the combined influence of lithology, structure, and humid tropical climate in shaping the pedogenic pathways of the Palakkad Gap (Sehgal, 1998; Bhattacharyya et al., 2009; Pal et al., 2014).

REFERENCE

Aleva, G. J. (1983). On Weathering and Denudation of Humid Tropical Interfluves and Their Triple Planation Surfaces. *Geologie en Mijnbouw, 62*(3), 383-388.

Balasubramaniam, K.S., & Sabale, S.G. (1984). Mineralogy, Geochemistry, and Genesis of Certain Bauxite Profiles from Kutch District, Gujarat. *Proceedings of Symposium on Deccan Trap and Bauxite. Special Publication. Geological Survey of India, 14*, 225–242.

Barshad, I. (1966, June). The Effect of a Variation in Precipitation on The Nature of Clay Mineral Formation in Soils from Acid and Basic Igneous Rocks. *In Proceedings of The International Clay Conference, 2*, 167-173. Israel Programme of Scientific Translation Jerusalem.

Bates, T. F. (1971). The Kaolin Minerals. In J. A. Gard (Ed.), *Mineralogical Society Monograph* (Vol. 3). Oxford: Aldren & Macaulay Ltd.

Bétard, F., Caner, L., Gunnell, Y. & Bourgeon, G. (2009) Illite Neoformation in Plagioclase During Weathering: Evidence from Semi-Arid Northeast Brazil. *Geoderma 152*, 53–62, https://doi.org/10.1016/j.geoderma.2009.05.016.

Bhattacharyya, R., Prakash, V., Kundu, S., Srivastva, A. K., & Gupta, H. S. (2009). Soil Aggregation and Organic Matter in A Sandy Clay Loam Soil of The Indian Himalayas Under Different Tillage and Crop Regimes. *Agriculture, Ecosystems & Environment, 132*(1-2), 126-134. https://doi.org/10.1016/j.agee.2009.03.007

Bhattacharyya, T., Pal, D. K., & Srivastava, P. (2000). Formation of Gibbsite in The Presence Of 2: 1 Minerals: An Example from Ultisols of Northeast India. *Clay Minerals, 35*(5), 827-840.

Birkeland, P. W. (1999). *Soils and Geomorphology* (3rd ed.). New York: Oxford University Press.

Brady, N. C., & Weil, R. R. (2008). *The Nature and Properties of Soils* (14th ed.). Pearson Prentice Hall.

Chamley, H. (1989). *Clay Sedimentology*. Berlin: Springer-Verlag.

Chandran, P., Ray, S. K., Bhattacharyya, T., Krishnan, P., & Pal, D. K. (2000). Clay Minerals in Two Ferruginous Soils of Southern India. *Clay Research 19*, 77–85.

Chandran, P., Ray, S. V., Bhattacharyya, T., Srivastava, P., Krishnan, P., & Pal, D. K. (2005). Lateritic Soils of Kerala, India: Their Mineralogy, Genesis, and Taxonomy. *Soil Research, 43*(7), 839-852. https://doi.org/10.1071/SR04128

Chattopadhyay S., & Chattopadhyay M. (1994). *Terrain Analysis of Kerala, Concept, Method and Application.* State Committee on Science, Technology and Environment, Government of Kerala.

Chipera, S. J., & Bish, D. L. (2013). Fitting Full X-ray Diffraction Patterns for Quantitative Analysis: A Method for Readily Quantifying Crystalline and Disordered Phases. *Advances in Materials Physics and Chemistry, 3*, 47-53 http://dx.doi.org/10.4236/ampc.2013.31A007

Collins, A. S., Clark, C., Sajeev, K., Santosh, M., Kelsey, D. E., & Hand, M. (2007). Passage Through India: The Mozambique Ocean Suture, High-Pressure Granulites And the Palghat-Cauvery Shear Zone System. *Terra Nova, 19*(2), 141-147. https://doi.org/10.1111/j.1365-3121.2007.00729.x

Cornell, R. M., & Schwertmann, U. (2003). *The Iron Oxides: Structure, Properties, Reactions, Occurrences, and Uses* (2nd ed.). Weinheim: Wiley-vch.

Corwin, D. L. (2021). Climate Change Impacts on Soil Salinity in Agricultural Areas. *European Journal of Soil Science, 72*(2), 842-862. https://doi.org/10.1111/ejss.13010

D'Cruz, E., Nair, P. K. R., & Prasannakumar, V. (2000) Palghat Gap—A Dextral Shear Zone from the South Indian Granulite Terrain. *Gondwana Research, 3*(1), 21–31. https://doi.org/10.1016/S1342-937X(05)70054-X

Deepthy, R., & Balakrishnan, S. (2005). Climatic Control on Clay Mineral Formation: Evidence from Weathering Profiles Developed on Either Side of The Western Ghats. *Journal of Earth System Science, 114*, 545-556. https://doi.org/10.1007/BF02702030

Dixon, J. B., & Schulze, D. G. (Eds.). (2002). *Soil Mineralogy with Environmental Applications*. Madison, WI: Soil Science Society of America.

Fernández-Caliani, J. C., Galán, E., Aparicio, P., Miras, A. & Márquez, M. G. (2010)

Origin and Geochemical Evolution of the Nuevo Montecastelo Kaolin Deposit (Galicia, NW Spain). *Applied Clay Science*, *49*(3), 91-97. https://doi.org/10.1016/j.clay.2010.06.006.

Gadgil, S. (2003). The Indian Monsoon and Its Variability. *Annual Review of Earth and Planetary Sciences*, *31*(1), 429–467. https://doi.org/10.1146/annurev.earth.31.100901.141251

Ganguli, S. S., Pal, S. K., Singh, S. L., Rama Rao, J. V., & Balakrishna, B. (2021). Insights into Crustal Architecture and Tectonics Across Palghat Cauvery Shear Zone, India from Combined Analysis of Gravity and Magnetic Data. *Geological Journal*, *56*(4), 2041-2059. https://doi.org/10.1002/gj.4041

Geiss, C. E., Egli, R., & Zanner, C. W. (2008). Direct Estimates of Pedogenic Magnetite as A Tool to Reconstruct Past Climates from Buried Soils. *Journal of Geophysical Research: Solid Earth*, *113*(B11). https://doi.org/10.1029/2008JB005669

Graham, R. C., Tice, K. R., & Guertal, W. R. (1994). The Pedologic Nature of Weathered Rock. *Whole Regolith Pedology*, *34*, 21-40. https://doi.org/10.2136/sssaspecpub34.c2

Hack, H. R. G. (2019). Weathering, Erosion, and Susceptibility to Weathering. In M. Kanji, E. A. B. Ferreira, & R. F. Azzoni (Eds.), *Soft Rock Mechanics and Engineering* (pp. 291–333). Springer International Publishing.

Hamed, H., Hale, W., & Stern, B. (2021). X-RAY Diffraction to Determine the Mineralogy in Soil Samples in the UK. *International Journal of Engineering Applied Sciences and Technology*, *5*(10), 91-98.

Hammond, E. H. (1964). Classes of Land Surface Form in the Forty-Eight States of the U.S.A. [Map supplement No. 4]. *Annals of the Association of American Geographers*, *54*(2), 11–19.

Harindranath, C. S., Venugopal, K. R., Raghu Mohan, N. G., Sehgal, J., & Velayutham, M. V. (1999). *Soils of Goa for Optimising Land Use* (NBSS Publ. 74b, Soils of India Series). National Bureau of Soil Survey and Land Use Planning, Nagpur, India.

Hemming, S. R. (2007). Paleoceanography, Physical and Chemical Proxies: Terrigenous Sediments. In S. A. Elias (Ed.), *Encyclopedia of Quaternary Science* (Vol. 3, pp. 1776–1785). Elsevier.

India Meteorological Department [IMD]. (2021, January 4). *Statement on Climate of India during 2020* [Press release]. Ministry of Earth Sciences, Government of India.

Jolicoeur, S., Ildefonse, P., & Bouchard, M. (2000). Kaolinite and Gibbsite Weathering of Biotite within Saprolites and Soils of Central Virginia. *Soil Science Society of America Journal, 64*(3), 1118-1129. https://doi.org/10.2136/sssaj2000.6431118x

Kahle, M., Kleber, M., & Jahn, R. (2002). Review of XRD-based Quantitative Analyses of Clay Minerals in Soils: the Suitability of Mineral Intensity Factors. *Geoderma*, *109*(3-4), 191-205. https://doi.org/10.1016/S0016-7061(02)00175-1

Karathanasis A. D., Johnson D. M. C & Matocha C. J. (2005). Biosolid Colloid-Mediated Transport of Copper, Zinc, and Lead in Waste Amended Soils. *Journal of Environmental Quality*, *34*(4), 1153-1164. https://doi.org/10.2134/jeq2004.0403

Kemp, R. A. (1985). The cause of redness in some buried and non-buried soils in eastern England. *Journal of Soil Science*, *36*(3), 329-334. https://doi.org/10.1111/j.1365-2389.1985.tb00339.x

Kharche, V. K. (1996). *Developing Soil-Site Suitability Criteria for Some Tropical Plantation Crops* (Doctoral dissertation, [Akola, Maharashtra, India]: Dr. Panjabrao Deshmukh Krishi Vidyapeeth).

Lal, R. (2008). Carbon Sequestration. *Philosophical Transactions of the Royal Society B: Biological Sciences*, *363*(1492), 815-830. https://doi.org/10.1098/rstb.2007.2185.

Liu, H., Chen, T., & Frost, R. L. (2014). An Overview of The Role of Goethite Surfaces in The Environment. *Chemosphere*, *103*, 1-11. https://doi.org/10.1016/j.chemosphere.2013.11.065

Liu, Z. H. & Dreybrodt, W. (1997). Dissolution Kinetics of Calcium Carbonate Minerals

in H2O-O2 Solutions in Turbulent Flow: The Role of The Diffusion Boundary Layer and The Slow Reaction H2O+ CO2 → H++ HCO3-. *Geochimica et Cosmochimica acta, 61*(14), 2879-2889. https://doi.org/10.1016/S0016-7037(97)00143-9.

Moore, I. D., & Reynolds, J. F. (1997). *An Introduction to Terrain Analysis*. Chichester: Wiley.

Mukherjee, S. (2022). Soil Minerology. In *Current Topics in Soil Science: An Environmental Approach* (pp. 11-18). Cham: Springer International Publishing.

Natarajan, A., Reddy, P. S. A., Sehgal, J., & Velayutham, M. (1997). *Soil Resources of Tamil Nadu for Land Use Planning* (NBSS Publ. 46b, Soils of India Series, 88 pp. + 4 Sheets of Soil Map at 1:500,000 Scale). National Bureau of Soil Survey and Land Use Planning.

Ogg, C. M., & Baker, J. C. (1999). Pedogenesis and Origin of Deeply Weathered Soils Formed in Alluvial Fans of The Virginia Blue Ridge. *Soil Science Society of America Journal, 63*(3), 601-606.

Ollier, C., & Pain, C. (1996). *Regolith, Soils and Landforms.* Chichester: Wiley.

Pal, D. K., Wani, S. P., Sahrawat, K. L., & Srivastava, P. (2014). Red Ferruginous Soils of Tropical Indian Environments: A Review of The Pedogenic Processes and Its Implications for Edaphology. *Catena, 121*, 260-278. https://doi.org/10.1016/j.catena.2014.05.023

Peucat, J. J., Vidal, P., Bernard-Griffiths, J., & Condie, K. C. (1989). Sr, Nd, and Pb Isotopic Systematics in the Archean Low- to High-Grade Transition Zone of Southern India: Syn-Accretion vs. Post-Accretion Granulites. *The Journal of Geology, 97*(5), 537-549. https://doi.org/10.1086/629333

Pike, R. J., & Wilson, S. E. (1971). Elevation Relief Ratio, Hypsometric Integral, and Geomorphic Area Altitude Analysis. *Bulletin of the Geological Society of America, 82*(4), 1079–1084. https://doi.org/10.1130/0016-7606(1971)82[1079:ERHIAG]2.0.CO;2

Pisharoty, P. R., & Asnani, G. C. (1957). Rainfall around monsoon depressions over India. *Indian Journal of Meteorology and Geophysics, 8*(1), 15–20. https://doi.org/10.54302/mausam.v8i1.4987.

Potter, M. J. (2000). Vermiculite. In *U.S. Geological Survey Minerals Yearbook* (pp. 83.81–83.82). U.S. Geological Survey.

Ravindrakumar, G.R. & Chacko,T (1994) Geothermobarometry of Mafic Granulites and Metapelite from The Palghat Gap, South India: Petrological Evidence for Isothermal Uplift and Rapid Cooling. *Journal of Metamorphic Geology, 12*(4), 479-492. https://doi.org/10.1111/j.1525-1314.1994.tb00037.x

Richards, L. A. (1954). *Diagnosis and Improvement of Saline and Alkali Soils* (U.S. Department of Agriculture Agricultural Handbook No. 60, 160 pp.). Washington, DC: U.S. Department of Agriculture.

Rothacker, L., Dosseto, A., Francke, A., Chivas, A. R., Vigier, N., & Kotarba-Morley, A. M., & Menozzi, D. (2018). Impact of Climate Change and Human Activity on Soil Landscapes Over The Past 12,300 Years. *Scientific Reports, 8*(1), 247. https://doi.org/10.1038/s41598-017-18603-4

Santosh, M., Tsunogae, T., & Koshimoto, S. (2004). First Report of Sapphirine-Bearing Rocks from the Palghat-Cauvery Shear Zone System, Southern India. *Gondwana Research, 7*(2), 620-626. https://doi.org/10.1016/S1342-937X(05)70813-3

Sehgal, J. L. (1998). Red and Lateritic Soils: An overview. In J. Sehgal, W. E. Blum, & K. S. Gajbhiye (Eds.), *Red and Lateritic Soils: Managing Red and Lateritic Soils for Sustainable Agriculture* (Vol. 1, pp. 3–10). Oxford & IBH Publishing, New Delhi.

Shiva Prasad, C. R., Reddy, P. S. A., Sehgal, J., & Velayutham, M. (1998). *Soils of Karnataka for Optimising Land Use* (NBSS Publ. 47b, Soils of India Series, 111 pp. + 4 Sheets of Soil Map at 1:500,000 Scale). National Bureau of Soil Survey and Land Use Planning, Nagpur, India.

Soil Survey Staff. (2014). Keys to Soil Taxonomy (12th ed.). U.S. Department of

Agriculture, Natural Resources Conservation Service.

Stoops, G., & Schaefer, C. E. (2018). Pedoplasmation: Formation of Soil Material. In G. Stoops, V. Marcelino, & F. Mees (Eds.), *Interpretation of Micromorphological Features of Soils and Regoliths* (pp. 59–71). Elsevier.

Subramanian, K. S., & Muraleedharan, M. P. (1985). Origin of the Palghat Gap in South India-A Synthesis. *Geological Society of India, 26*(1), 28-37. https://doi.org/10.17491/jgsi/1985/260104

Varghese, T., & Byju, G. (1993). *Laterite Soils* (Technical Monograph No. 1). State Committee on Science, Technology and Environment, Government of Kerala, Kerala, India.

Verstappen, H. T. (1983). *Applied geomorphology: Geomorphological Surveys for Environmental Development*. Amsterdam: Elsevier.

Tait, J. M., Violante, A., & Violante, P. (1983). Co-crystallization of Gibbsite and Bayerite with Nordstrandite. *Clay Minerals, 18*(1), 95-99. https://doi.org/10.1180/claymin.1983.018.1.09

Tazaki, K. A. Z. U. E. (1976). Scanning Electron Microscopic Study of Formation of Gibbsite from Plagioclase. *Institute for Thermal Spring Research, 45*, 11-24.

Van der Merwe, C. R. & H. W. Weber. (1963). The clay minerals of South African soils developed from granite under different climatic conditions. *South African Journal of Agricultural Science, 6*(3), 411-454.

Velmurugan, A., Swarnam, T. P., Ambast, S. K., & Kumar, N. (2016). Managing Waterlogging and Soil Salinity with A Permanent Raised Bed and Furrow System in Coastal Lowlands of Humid Tropics. *Agricultural Water Management, 168*, 56–67. https://doi.org/10.1016/j.agwat.2016.01.020

Wang, C., Ross, G. J., & Rees, H. W. (1981). Characteristics of Residual and Colluvial Soils Developed on Granite and of The Associated Pre-Wisconsin Landforms in North-Central New Brunswick. *Canadian Journal of Earth Sciences, 18*(3), 487-494. https://doi.org/10.1139/e81-042

Wang, Q., Wang, W., He, X., Zheng, Q., Wang, H., Wu, Y., & Zhong, Z. (2017). Changes in Soil Properties, X-ray-mineral Diffractions and Infrared-Functional Groups in Bulk Soil and Fractions Following Afforestation of Farmland, Northeast China. *Scientific Reports, 7*(1), 12829. https://doi.org/10.1038/s41598-017-12809-2

Wang, X., Zhang, M., Zhang, W., Wang, J., Zhou, Y., Song, X., Li, T., Li, X., Liu, H., & Zhao, L. (2012). Occurrence and Origins of Minerals in Mixed-Layer Illite/Smectite-Rich Coals of the Late Permian Age from the Changxing Mine, Eastern Yunnan, China. *International Journal of Coal Geology, 102*, 26-34. https://doi.org/10.1016/j.coal.2012.07.010

Wilson, M. J. (1999). The Origin and Formation of Clay Minerals in Soils: Past, Present and Future Perspectives. *Clay Minerals, 34*(1), 7–25. https://doi.org/10.1180/000985599545957

Zhou, X., Liu, D., Bu, H., Deng, L., Liu, H., Yuan, P., Du, P., & Song, H. (2018). XRD-Based Quantitative Analysis of Clay Minerals Using Reference Intensity Ratios, Mineral Intensity Factors, Rietveld, and Full Pattern Summation Methods: A Critical Review. *Solid Earth Sciences, 3*(1), 16-29. https://doi.org/10.1016/j.sesci.2017.12.002